

# Seismic risk assessment of transportation utilities in Jammu and Kashmir

Abdullah Ansari (✉ [aamomin183@gmail.com](mailto:aamomin183@gmail.com))

Indian Institute of Technology Delhi

KS Rao

Indian Institute of Technology Delhi

AK Jain

Indian Institute of Technology Delhi



---

## Research Article

**Keywords:** Seismic risk, USBRL, Jammu and Kashmir, Railway track, Himalayas, Tunnelling

**Posted Date:** January 25th, 2023

**DOI:** <https://doi.org/10.21203/rs.3.rs-2503269/v1>

**License:**   This work is licensed under a Creative Commons Attribution 4.0 International License. [Read Full License](#)

---

# Abstract

Regarding passenger safety and road serviceability, the effects of earthquakes on underground transportation systems situated in seismically active regions yield a great challenge. The 345 km long Udhampur Srinagar Baramulla Rail Link (USBRL) project in Jammu and Kashmir is a railway track with underground tunnels that traverses the tectonically active area of the northwestern part of the Himalayas under difficult geological conditions. In this study, the Semi-Quantitative Seismic Risk Assessment (SQ-SRA) approach has been used to evaluate the seismic risk and post-seismic serviceability of this project. Out of the three alignment phases, the first one is accessible, the center one is accessible but requires repair, and the last one is inaccessible, according to the risk matrices. The majority of the tunnel sections in the last phase are situated near zones prone to landslides and large tectonic sources, and they also include extensively weathered rock mass, resulting in deformation, squeezing and cavity formation during the excavation process. The progressive effect of these issues increases the probability that these tunnels may get extensive damage, which would render the track segment inoperable under post-seismic conditions. The risk matrices and maps provided will serve as a valuable tool for directing track operations.

## 1. Introduction

The development and progress of any region require a well-established transportation network as a prerequisite for overall economic growth. For the best possible use of the resources, it is crucial to integrate the growth of multiple transport modes. But natural disasters like earthquakes, tsunamis, floods, avalanches, etc. have put a negative impression on the performance of the transportation networks during post-disaster scenarios. The roadway and railway are the two most convenient modes of transportation. The availability of space is a major mishap for the establishment of such networks. To overcome this, underground spacing is an outstanding alternative and this leads to an increase in the demand for tunnel construction. Unfortunately, tunnels and associated infrastructure damages due to the 1995 Kobe earthquake in Japan, the 1999 Chi-Chi earthquake in Taiwan, the 2008 Wenchuan earthquake in China, and the 2016 Kumamoto earthquake in Japan discarded the belief in the structural safety of underground structures during seismic events (Mwafy and Elnashai 2002; Cilingir and Madabhushi, 2011; Mazars et al. 2011; Su et al., 2017; Jsayalakshmi et al. 2018; Tsindis et al., 2020; Mirzanejad et al. 2021; Wang et al., 2021; Ansari et al. 2022d). Tunnel damages from previous earthquakes in developed countries have shown that tunnels are vulnerable to strong seismic motion as well, and even minor damage can result in significant losses. Tunnels are built as part of infrastructure projects or upgraded transportation networks (Beghoul et al. 2010; Wang et al. 2019; Rajput et al. 2022). Any seismic damage to them might disrupt the overall serviceability of road or railway transit, causing socioeconomic disruption and perhaps disastrous outcomes.

Jammu and Kashmir (J&K) is located in the Northwestern part of the Himalayan region and is frequently triggered by moderate to large magnitude earthquakes. The major earthquakes provoked in 1555, 1828, 1885, 1905, and 2005. The; 2005 Kashmir earthquake ( $M_w=7.6$ ) was one of the worst, with over 0.1 million people killed and infrastructure projects including bridges, retaining walls, and dams destroyed. Along the

route between Murree and Muzaffarabad, there was just one roadway tunnel damaged (Mwafy and Elnashai 2001; Durrani et al., 2005; Choun and Elnashai 2010; Xie et al. 2011; Hashash et al. 2012; Sahana and Sajjad, 2017; Ansari et al. 2022b). The growing Udhampur Srinagar Baramulla Rail Link (USBRL) project in this area, together with the previous historical record of earthquakes and seismotectonic settings push to examine the seismic risk of railway tunnels and the serviceability of different phases during post-seismic scenarios. Recently occurred far-field June 2022 Paktika earthquake ( $M_w=5.9$ ) in Afghanistan and the 2019 Mirpur earthquake ( $M_w=5.6$ ) in Pakistan are also showing the active dynamics of the tectonic plates in the Himalayan belt.

The alignment of the USBRL project track and neighbouring active tectonic sources are shown in Fig. 1. Srinagar and Jammu are the two capital cities of J&K. Srinagar is functional during summer while all administrative activities are handled from Jammu during the winter session. The National Highway 1A (NH1A) is the main transportation source to reach Srinagar from Jammu. This highway faces frequent landslides due to poor geological conditions and resulting in heavy traffic jams (Fig. 2a). The Mughal Road route cuts the distance between Shopian and Poonch from 588 km to 126 km and links Rajouri and Poonch of Jammu Region (JR) to Srinagar in the KV. The Government of India has declared the USBRL project a "Project of National Importance". The main aim of this project is to connect the Kashmir Valley (KV) with Mainland India in all circumstances. When this project is finished, J&K will have dependable, all-weather access to the rest of the nation via the railway network, as well as access by train to remote districts. Approach roads to construction sites will be built for a total of around 262 km. Over 73 villages will be connected after approach roads are finished, giving a half million people access to roadways. The military, army, and border force personnel will be able to handle any emergency scenarios through this railway route. The cheaper mode of transportation, formulation of the new industrial hub, and employment generation are the core benefits of this project. This is providing wonderful employment opportunities to the local people. It will support the overall growth and development of the region. The Udhampur and Baramulla are the starting and ending railway stations of this track which connect the cities like Reasi, Ramban, Anantnag, Srinagar, Shopian, and Pulwama. People residing in remote areas like Kishtwar, Ramban, Pulwama, and Shopian can access this route to reach Shaikh Ul Alam International Airport in Srinagar for international travel. The tourism business will flourish, especially for visitors to popular destinations like Pahalgam, Gulmarg, Sonmarg, Doodhpathri, Betab Valley, and Aru Valley. These locations are already drawing tourists from all over the world because of the natural splendour of KV.

In the present study, an attempt has been done to assess the seismic risk and post-seismic serviceability of the USBRL project. The semi-Quantitative Seismic Risk Assessment (SQ-SRA) approach is employed to decide on the functionality of selected phases along the railway track alignment. Several critical geological phenomena, such as cavity development, face wall deformation, squeezing, chimney formation, and water leakages, were seen in Tunnels T2, T5, T40/41, T50, and T74R. The presence of these issues and the high degree of seismicity of the region increase the chances of portal and lining damages. The probability of portal and lining damages is increased by the existence of these problems and the high level of seismic activity in the area. The probabilities of various modes of damage for all tunnels are audited through fragility functions considering Peak Ground Acceleration (PGA) as seismic intensity measure. The risk

matrices are formed as outcomes of SQ-SRA which predict the risk in terms of health, safety, and operation. Based on the tectonic environment, tunnel typology, and structural integrity, the three Phases (P1, P2, and P3) of the railway tracks are found to be accessible, accessible with moderate repair, and inaccessible. P1 and P2 seem to be operational, however, P3 is absolutely inaccessible. Phase 3 is the riskiest track in terms of post-seismic functioning because of the consequences of a high degree of seismicity, landslide susceptibility, weathered rock mass, and near-source characterisation.

## **2. Geological And Tectonic Attributes**

The USBRL project is located in the NW Himalayas, especially in the Lesser Himalaya Zone, from a regional geological standpoint. The Main Central Thrust (MCT) in the north and the Main Boundary Thrust (MBT) in the south define the Lesser Himalayan Zone. The lower Himalaya's geological unit is mostly made up of sedimentary rocks that have been sheared and over-thrust to the south into the Siwalik Molasse (Sub-Himalaya Zone) following the NNE dipping Reasi Thrust (RT). The major geological formations present in the Southwestern part of J&K are mentioned in Table 1.



Table 1  
Geological formations and lithounits in the southwestern part of Jammu and Kashmir

<b>Geological Formation</b>	<b>Description</b>
Indus-Alluvium	Paleo-Neogene sedimentary succession makes up this frontal Cenozoic Sub-Himalayan foreland basin (Jain et al. 2009; Ansari et al. 2022f). The southern boundary of the JR including the bank of the Tawi River in the Samba and Kathua area exposes the alluvial plains (Fig. 3a).
Siwaliks	North of the Indus Alluvium, the Siwaliks are exposed and may be separated into three sub-groups: the Upper Siwaliks, Middle Siwaliks, and Lower Siwaliks (Fig. 3b).
Sirban Formation	Near Reasi and Vaishnodevi, this formation is mostly visible (Siddaiah 2011). The formation comprises dark grey dolomite and limestone with a back thrust concerning the overlying Subathu Formation (Fig. 3c). The upper part is known as Khairikot Formation while the lower one is named Trikuta Formation
Subathu Formation	Subathu Formation comprising the oldest beds of the Himalayan Foreland Basin occurs in the NW Himalayas, which unconformably overlies Pre-Cambrian rocks (Siddaiah and Kumar 2007).
Murre Formation	After a considerable time interval, the fine-grained detrital sediments of the Murree Formation (Mehta and Jolly 1989; Mohanty et al. 2022) were deposited above the Subathu Formation (Shah 1977). The iron staining may be seen on this reddish rock formation. In the JR, MBT is known as Murre Thrust (MT), which originates from Murre, a town in Pakistan. This thrust places the Lesser Himalayan sequences over the tertiary sedimentary strata of Siwaliks. In Tunnel T47, the contact between Murre Formation and Ramban Formation has been observed at 20 m (Fig. 3e) from the North Portal which directly indicates the presence of MT (Wani and Alamgir 2017; Ahmad et al. 2021; Ansari et al 2022f).
Ramban Formation	This formation is also known as the Dogra Formation which is a member of the Carboniferous-Eocene Autochthonous Folded Belt (Wadia 1931). The Panjal Volcanics and the Upper Palaeozoic to Lower Tertiary Agglomeratic Slate Sequence are unconformably overlain by this formation (Jangpangi et al. 1986). Slate, phyllite, quartzite, and gneiss are the main rocks that make up this formation. The Panjal Thrust (PT) is the MCT in this area and passes sthrough the Ramban and some part of Reasi (Fig. 3d).
Salkhala Formation	The formation is bordered to the south by the PT and to the west and east, respectively, by the Sincha Formation and Bhadarwah Formation (Thakur 1998). Rocks of the Salkhala Formation constitute a low to high-grade meta-sedimentary suite comprising phyllite, schist, quartzite, and limestone (Fig. 3f).

The JR has been impacted due to the near-field as well as far-field earthquakes in the Himalayan region extending up to Hindukush in Afghanistan (Singh and Mishra, 2004; Lister et al. 2008; Aslam et al. 2021; Ansari et al. 2022f). The Jhelum Fault (JF), Attock Fault (AF), Reasi Fault (RF), Balakot-Bagh Fault (BBF), Deosai Fault (DF), Jwalamukhi Thrust Jwalamukhi Thrust Hanna Fault (HF), Batal Fault (BF), and Mawer Fault (MF) are few of the active faults that surround this area (Bilham and Wallace 2005). The MCT distinguishes the crystalline rocks of the higher Himalayas from the formations of the lower Himalayas (Gupta and Gahalaut 2014). Along the JR's northern boundary, the MBT) and PT run parallel. NNW-SSE and NW-SE trends are shown by the Jwalamukhi Thrust (JT) and Balapur Thrust (BT) respectively (Malik and Mohanty 2007; Alam et al. 2015; Sana and Nath 2017; Mittal et al. 2021). The NE dipping Kishtwar

Fault (KF) and the NS trending Jhelum Fault (JF) are the two major local strike-slip faults in the JR. The BBF, which is NE dipping in Pakistan, is the primary cause of the 2005 Muzaffarabad earthquake (Avouac et al. 2006; Pathier et al. 2006). Active R and Udhampur Fault Zone (UFZ) pass through the core center section of the JR in addition to the MBT. As a result of the imbrication of the lower Himalayas into a deeper structural level, the Kishtwar Window (KW) developed inside the crystalline upper Himalayas (Singh 2010; Pandey et al. 2017; Romshoo, et al., 2018; Pandita et al. 2021). The major tectonic features along with earthquake epicenters having magnitude  $M_w \geq 4.0$  are shown in the following Fig. 4.

## **3. Transportation Projects In Jammu And Kashmir**

### **3.1 USBRL Project details**

The main concept behind the proposal of the USBRL project is to work on the traffic issues in the Jammu and Kashmir. The Indian government proposed a 345 km long railway line connecting the Kashmir Valley with the Indian Railways network to offer J&K an easy way of transportation option (Kumar et al. 2021; Ansari et al. 2021a; Ansari et al. 2022f). The construction of a new railroad line in the Indian subcontinent has never been more challenging than this one. The young Himalayas that is full of geological surprises and myriad issues are traversed by the terrain. The project has been divided into 4 subsections for execution purposes. The alignment and structural details for each subsection are mentioned in Table 2.

Table 2  
Comprehensive detailing of the subsections of the USBRL project.

Parameters	Subsections			
	Udhampur-to-Katra (UD-KT)	Katra-to-Banihal (KT-BN)	Banihal-to-Quazigund (BN-QZ)	Quazigund-to-Baramulla (QZ-BR)
Executing Agency	Northern Railways	Northern Railways, Konkan Railway Corporation Limited (KRCL), and Ircon International	Northern Railways, Konkan Railway Corporation Limited (KRCL), and Ircon International	Ircon International
Completion Cost (In Crores)	1111	21821	1992	3430
Cost per km (In Crores)	44	194	94	30
Total Stations	3	10	1	15
Route length (km)	25	111	18	118
Maximum Curvature	5°	4.86°	3.1°	2.75°
<b>Tunnels</b>				
Total Tunnels	10	27	1	0
Length (km)	11	164	11.21	0
Percentage Length in Tunnel (%)	44	87	62	
<b>Bridges</b>				
Total Bridges	50	37	35	809
Length (km)	1.48	7.035	0.28	4.21

The Chenab Bridge and Anji Bridge are located in the Reasi and are the two main bridges under the subsection between Katra to Banihal. The Chenab Bridge is one of the engineering marvel structures in Reasi. Considering the geology including jointed, weathered, and weak Himalayan rocks and geopolitical issues, it is designed to resist earthquakes, fire, impact as well as blast loads. The bridge over the Chenab River might have been built at a lower height, according to the engineers (Ansari et al. 2021; Dewan et al.

2022). However, the elevation is raised to 359 m above the riverbed, which is around 35 m higher than the Eiffel tower in Paris, to avoid the steep slope between the Banihal station and Chenab Bridge (Fig. 2d). The Anji Khad Bridge (Fig. 2e) is the first cable-stayed bridge by the Indian Railways located in Reasi which acts as a connecting chain between Tunnel T2 (Fig. 2b and Fig. 2c) and Tunnel T3. The main features of these two bridges are highlighted in Table 3.

Table 3  
Parametric characteristics of main bridges in Katra-Banihal (KT-BN) subsection.

Parameters	Detailing	
	Chenab Bridge	Anji Khad Bridge
Bridge length	1315 m	657 m
Continuous Deck Length of Viaduct	785 m	240 m
Continuous Span Length over Arch	530 m	417 m
Steel Deck Width	17 m	13.5 m
Height above the riverbed	359 m	196 m
Seismic Zone (BIS Zonation)	Zone V	Zone V

Most of the tunnels under this project are located near the major tectonic sources including MBT, MCT, PT, and BT. The Tunnels T2, T49, and T80 are the main tunnels of this route. The total length of Tunnel T49 is 12.75 km which is going to become India's longest tunnel. The Tunnel T80 is known as the Pir Panjal tunnel passing through the Pir Panjal ranges and acts as a gateway to KV. This is the only tunnel in Banihal to Quazigund (BN-QZ) subsection with maximum overburden of 1300 m. Because earthquakes are likely to strike anywhere within the tunnel structure, the distances between all conceivable locations and the nearest tectonics sources are considered. Table 4 enlist the structural integrity of selected tunnel sections and expected seismic hazard for the surrounding environment.

Table 4

List of major tunnel sections under USBRL project with structural and seismic parameters considered for the risk assessment.

Tunnel	Fault/Thrust	SSD (km)	Fault Length (km)	PGA <sub>max</sub>	Section	M <sub>obs</sub>	Total Tunnel Length (m)	Overburden Depth (m)
T44/45P1.2	MBT	4.8	325.25	0.711	KT-BN	7.8	1483	575
T44/45P2.2	MBT	5.3	325.25	0.711	KT-BN	7.8	1483	877
T46P2.2	MBT	6.3	325.25	0.711	KT-BN	7.8	654	256
T5P2.3	RT	6.4	163.08	0.831	KT-BN	6.3	5959	359
T5P1.3	RT	6.8	163.08	0.831	KT-BN	6.3	5959	387
T46P1.2	MBT	7.4	325.25	0.711	KT-BN	7.8	654	456
T46P1.3	PT	8.2	274.53	0.343	KT-BN	5.5	654	367
T46P2.3	PT	8.3	274.53	0.343	KT-BN	5.5	654	367
T42/43P1.2	MBT	10.1	325.25	0.711	KT-BN	7.8	2732	256
T42/43P1.1	MCT	10.3	91.41	0.821	KT-BN	7.8	2732	245
T42/43P2.1	MCT	10.7	91.41	0.821	KT-BN	7.8	2732	357
T42/43P2.2	MBT	11.3	325.25	0.711	KT-BN	7.8	2732	578
T40/41P1.2	MBT	11.5	325.25	0.711	KT-BN	7.8	1340	245
T40/41P2.2	MBT	11.8	325.25	0.711	KT-BN	7.8	1340	788
T44/45P1.1	MCT	11.8	91.41	0.821	KT-BN	7.8	1483	377
T74RP1.1	MCT	11.9	91.41	0.821	KT-BN	7.8	8600	130
T40/41P1.1	MCT	12.1	91.41	0.831	KT-BN	7.8	1340	422
T44/45P2.1	MCT	12.1	91.41	0.821	KT-BN	7.8	1483	459
T46P1.1	MCT	12.1	91.41	0.821	KT-BN	7.8	654	256
T40/41P2.1	MCT	12.4	91.41	0.821	KT-BN	7.8	1340	367
T74RP2.1	MCT	12.5	91.41	0.821	KT-BN	7.8	8600	130
T46P2.1	MCT	12.8	91.41	0.821	KT-BN	7.8	654	457
T15P2.1	MCT	16.8	91.41	0.821	KT-BN	7.8	9810	656
T23P1.2	JT	16.9	245.86	0.69	UD-KT	7.8	1800	119
T15P1.1	MCT	17.1	91.41	0.821	KT-BN	7.8	9810	398

Tunnel	Fault/Thrust	SSD (km)	Fault Length (km)	PGA <sub>max</sub>	Section	M <sub>obs</sub>	Total Tunnel Length (m)	Overburden Depth (m)
T14P2.1	MCT	17.5	91.41	0.821	KT-BN	7.8	3142	877
T14P1.2	MBT	17.8	325.25	0.711	KT-BN	7.8	3142	456
T14P2.4	RT	17.8	163.08	0.831	KT-BN	6.3	3142	376
T74RP1.2	MBT	17.8	325.25	0.711	KT-BN	7.8	8600	654
T14P1.1	MCT	18.5	91.41	0.821	KT-BN	7.8	3142	343
T74RP2.2	MBT	18.8	325.25	0.711	KT-BN	7.8	8600	654
T13P2.1	MCT	22.7	91.41	0.821	KT-BN	7.8	9370	150
T13P1.2	MBT	22.9	325.25	0.711	KT-BN	7.8	9370	235
T12P2.2	MBT	23.1	325.25	0.711	KT-BN	7.8	2123	467
T11P1.2	MBT	23.2	325.25	0.711	KT-BN	7.8	830	543
T12P1.2	MBT	23.2	325.25	0.711	KT-BN	7.8	2123	873
T15P1.2	MBT	23.2	325.25	0.711	KT-BN	7.8	9810	572
T14P1.3	PT	23.4	274.53	0.343	KT-BN	5.5	3142	354
T11P2.2	MBT	23.6	325.25	0.711	KT-BN	7.8	830	462
T23P1.1	RT	23.7	163.08	0.831	UD-KT	7.8	1800	230
T25P1.1	RT	23.8	163.08	0.831	UD-KT	7.8	2500	385
T15P2.2	MBT	24.1	325.25	0.69	KT-BN	7.8	9810	632
T14P2.2	MBT	24.2	325.25	0.711	KT-BN	7.8	3142	687
T25P2.1	RT	24.3	163.08	0.831	UD-KT	7.8	2500	196
T5P1.2	JT	24.7	245.86	0.69	KT-BN	7.8	5959	381
T5P2.2	JT	24.9	245.86	0.69	KT-BN	7.8	5959	277
T10P2.2	MBT	25.4	325.25	0.711	KT-BN	7.8	970	242
T25P1.2	JT	25.4	245.86	0.69	UD-KT	7.8	2500	196
T23P2.1	RT	25.5	163.08	0.831	UD-KT	7.8	1800	230
T13P1.4	RT	25.7	163.08	0.831	KT-BN	6.3	9370	235
T10P1.2	MBT	25.8	325.25	0.711	KT-BN	7.8	970	644

Tunnel	Fault/Thrust	SSD (km)	Fault Length (km)	PGA <sub>max</sub>	Section	M <sub>obs</sub>	Total Tunnel Length (m)	Overburden Depth (m)
T13P2.4	RT	25.8	163.08	0.831	KT-BN	6.3	9370	322
T13P2.3	PT	26.2	274.53	0.343	KT-BN	5.5	9370	298
T23P2.2	JT	26.4	245.86	0.69	UD-KT	7.8	1800	119
T6P1.2	MBT	26.5	325.25	0.711	KT-BN	7.8	3493	355
T6P2.2	MBT	26.7	325.25	0.711	KT-BN	7.8	3493	378
T6P1.3	PT	26.8	274.53	0.343	KT-BN	5.5	3493	785
T5P1.1	MBT	27.7	325.25	0.711	KT-BN	7.8	5959	378
T5P2.1	MBT	27.8	325.25	0.711	KT-BN	7.8	5959	295
T6P2.3	PT	28.2	274.53	0.343	KT-BN	5.5	3493	478
T10P1.3	PT	28.7	274.53	0.343	KT-BN	5.5	970	325
T14P1.4	RT	28.7	163.08	0.831	KT-BN	6.3	3142	673
T14P2.3	PT	28.8	274.53	0.343	KT-BN	5.5	3142	327
T25P2.2	JT	28.8	245.86	0.69	UD-KT	7.8	2500	231
T10P2.3	PT	29.1	274.53	0.343	KT-BN	5.5	970	455
T13P1.1	MCT	29.4	91.41	0.821	KT-BN	7.8	9370	150
T12P2.1	MCT	29.7	91.41	0.821	KT-BN	7.8	2123	367
T12P1.1	MCT	29.8	91.41	0.821	KT-BN	7.8	2123	746
T11P1.3	PT	30.1	274.53	0.343	KT-BN	5.5	830	435
T11P2.3	PT	30.5	274.53	0.343	KT-BN	5.5	830	367
T11P2.1	MCT	30.7	91.41	0.821	KT-BN	7.8	830	467
T11P1.1	MCT	30.9	91.41	0.821	KT-BN	7.8	830	533
T12P1.3	PT	31.1	274.53	0.343	KT-BN	5.5	2123	356
T6P1.1	MCT	31.2	91.41	0.821	KT-BN	7.8	3493	566
T10P1.1	MCT	31.3	91.41	0.821	KT-BN	7.8	970	743
T10P2.1	MCT	31.7	91.41	0.821	KT-BN	7.8	970	535
T12P2.3	PT	31.7	274.53	0.343	KT-BN	5.5	2123	577

Tunnel	Fault/Thrust	SSD (km)	Fault Length (km)	PGA <sub>max</sub>	Section	M <sub>obs</sub>	Total Tunnel Length (m)	Overburden Depth (m)
T6P2.1	MCT	32.1	91.41	0.821	KT-BN	7.8	3493	367
T13P1.3	PT	32.1	274.53	0.343	KT-BN	5.5	9370	150
T13P2.2	MBT	32.2	325.25	0.711	KT-BN	7.8	9370	235
T2P1.1	RT	4.1	163.08	0.831	KT-BN	6.3	5160	235
T1P2.1	RT	4.2	163.08	0.831	KT-BN	6.3	3068	176
T1P1.1	RT	4.6	163.08	0.831	KT-BN	6.3	3068	104
T2P2.1	RT	5.2	163.08	0.831	KT-BN	6.3	5160	366
T3P1.1	RT	6.2	163.08	0.831	KT-BN	6.3	3009	105
T47P1.2	MBT	7.3	325.25	0.711	KT-BN	7.8	2230	567
T3P2.1	RT	7.6	163.08	0.831	KT-BN	6.3	3009	243
T47P2.2	MBT	7.8	325.25	0.711	KT-BN	7.8	2230	566
T50P2.1	MCT	7.9	91.41	0.821	KT-BN	7.8	255	1032
T50P1.1	MCT	8.9	91.41	0.821	KT-BN	7.8	255	864
T47P1.3	PT	9.2	274.53	0.343	KT-BN	5.5	2230	363
T47P2.3	PT	9.4	274.53	0.343	KT-BN	5.5	2230	677
T47P1.1	MCT	13.2	91.41	0.821	KT-BN	7.8	2230	357
T47P2.1	MCT	14.11	91.41	0.821	KT-BN	7.8	2230	467
T50P1.2	MBT	15.4	325.25	0.711	KT-BN	7.8	255	368
T80P1.2	BT	15.4	88.76	0.741	BN-QZ	7.6	10900	1320
T80P2.2	BT	15.8	88.76	0.741	BN-QZ	7.6	10900	1320
T50P1.3	PT	16.4	274.53	0.343	KT-BN	5.5	255	942
T50P2.2	MBT	16.4	325.25	0.711	KT-BN	7.8	255	765
T80P1.1	PT	17.1	274.53	0.343	BN-QZ	5.5	10900	1100
T80P2.1	PT	18.3	274.53	0.343	BN-QZ	5.5	10900	1100
T2P1.2	JT	18.7	245.86	0.69	KT-BN	7.8	5160	265
T50P2.3	PT	18.7	274.53	0.343	KT-BN	5.5	255	246



Tunnel	Fault/Thrust	SSD (km)	Fault Length (km)	PGA <sub>max</sub>	Section	M <sub>obs</sub>	Total Tunnel Length (m)	Overburden Depth (m)
T2P2.2	JT	18.9	245.86	0.69	KT-BN	7.8	5160	322
T1P2.2	JT	19.4	245.86	0.69	KT-BN	7.8	3068	123
T1P1.2	JT	19.6	245.86	0.69	KT-BN	7.8	3068	98
T77DP1.1	MCT	21.3	91.41	0.821	KT-BN	7.8	1760	454
T77DP1.2	MBT	21.9	325.25	0.711	KT-BN	7.8	1760	732
T3P1.2	JT	23.2	245.86	0.69	KT-BN	7.8	3009	210
T77DP2.1	MCT	23.3	91.41	0.821	KT-BN	7.8	1760	454
T80P1.3	MCT	23.5	91.41	0.821	BN-QZ	7.8	10900	1320
T1P1.3	MFT	23.6	198.05	0.33	KT-BN	6.7	3068	117
T77DP2.2	MBT	23.7	325.25	0.711	KT-BN	7.8	1760	732
T80P2.3	MCT	23.7	91.41	0.821	BN-QZ	7.8	10900	1320
T1P2.3	MFT	23.8	198.05	0.33	KT-BN	6.7	3068	165
T80P2.4	MBT	27.2	325.25	0.711	BN-QZ	7.8	10900	1320
T80P1.4	MBT	27.4	325.25	0.711	BN-QZ	7.8	10900	1320
T2P2.3	MFT	27.8	198.05	0.33	KT-BN	6.7	5160	189
T3P2.3	MFT	29.6	198.05	0.33	KT-BN	6.7	3009	245
T3P2.2	JT	31.1	245.86	0.69	KT-BN	7.8	3009	288
T2P1.3	MFT	32.2	198.05	0.33	KT-BN	6.7	5160	255
T3P1.3	MFT	32.2	198.05	0.33	KT-BN	6.7	3009	255
T2P2.5	MBT	32.9	325.25	0.711	KT-BN	7.8	5160	587
T2P1.4	MCT	33.8	91.41	0.821	KT-BN	7.8	5160	543
T2P2.4	MCT	34.2	91.41	0.821	KT-BN	7.8	5160	654
T2P1.5	MBT	38.1	325.25	0.711	KT-BN	7.8	5160	521
T49P1.1	MCT	7.3	91.41	0.821	KT-BN	7.8	12750	1033
T49P2.1	MCT	7.5	91.41	0.821	KT-BN	7.8	12750	335
T48P2.2	MBT	8.8	325.25	0.711	KT-BN	7.8	10180	672

Tunnel	Fault/Thrust	SSD (km)	Fault Length (km)	PGA <sub>max</sub>	Section	M <sub>obs</sub>	Total Tunnel Length (m)	Overburden Depth (m)
T48P1.2	MBT	9.6	325.25	0.711	KT-BN	7.8	10180	862
T49P2.2	MBT	13.3	325.25	0.711	KT-BN	7.8	12750	789
T49P1.2	MBT	13.6	325.25	0.711	KT-BN	7.8	12750	1105
T49P1.3	PT	13.8	274.53	0.343	KT-BN	5.5	12750	1008
T49P2.3	PT	14.1	274.53	0.343	KT-BN	5.5	12750	932
T78P1.1	MCT	14.3	91.41	0.821	KT-BN	7.8	920	758
T78P2.1	MCT	15.2	91.41	0.821	KT-BN	7.8	920	758
T78P1.2	MBT	16.7	325.25	0.711	KT-BN	7.8	920	639
T78P2.2	MBT	17.2	325.25	0.711	KT-BN	7.8	920	639
T48P1.3	PT	18.2	274.53	0.343	KT-BN	5.5	10180	783
T48P2.1	MCT	18.6	91.41	0.821	KT-BN	7.8	10180	356
T48P1.1	MCT	18.7	91.41	0.821	KT-BN	7.8	10180	363
T48P2.3	PT	19.3	274.53	0.343	KT-BN	5.5	10180	933

*\* Here, SSD = Source to Site Distance, MCT = Main Central Thrust, MBT = Main Boundary Thrust, RT = Reasi Thrust, BT = Balapur Thrust, JT = Jhelum Thrust, UD-KT = Udampur to Katra, KT-BN = Katra to Banihal, BN-QZ = Banihal to Quazigund.*

## 3.2 Challenges in Himlayan terrain

The Himalayas have the world's most difficult ground conditions from the standpoint of tunnelling. One of the prime reasons for this is that they are the youngest of the mountain chains. The Tunnel T2 is 5.09 km long and runs between Pie Khad and Anji Khad in Reasi (Fig. 2f). The whole length of the tunnel is made up of rocks from the Sirban Group's Trikuta Formation (Fig. 5). The rock mass is made up of jointed cherty dolomite with shale or slate interlayers. During the excavation, a cavity or collapse occurred at the top part of the tunnel, accompanied by a massive rush of water and fractured rock mass. As shown in the following Fig. 6, the rock mass encountered at the North Portal has been represented by two lithological units separated by a gouge-filled shear zone of 10–15 cm. The shear zone is first encountered at the right side of the face and is moving towards the left side with the advancement of the excavation. The rock mass at the left side of the tunnel face consists of black shale or slate which is thinly bedded, weak in nature, and highly jointed. On the right side of the face, the rock mass encountered is fragmented dolomite which is weak to medium strong and smooth to slightly rough. Steps taken to handle the problem of cavity formation are explained in the following Table 5.

Table 5  
Measures taken to grasp the cavity formation in Tunnel T2.

Action Plan	Description
Plugging	To handle the flow of loose debris material, the whole face of the tunnel was filled with it. To verify the flowing material, the face was sealed with external muck and sand-filled bags. Wire mesh and shotcrete were given in addition to the vertical dowel bars.
Drainage Holes	Drainage holes for a length of 6m to 9m with a diameter of 76 mm are given at the crown part by inserting perforated pipes after the face has been completely plugged.
Pipe Roofing	At the crown, two layers of perforated pipes with a length of 12 m and a diameter of 114.3 mm are inserted at various angles with a center-to-center spacing of 15 to 20 cm. The pipes are perforated with 5 mm diameter holes spaced 30 cm apart. To support the pipes, a dummy rib was built at the crown. Pipes are put at an angle of 30° to 35° degrees in the first layer, and 6° to 10° degrees in the second layer, and are entirely grouted.
Consolidation Grouting	After proper pipe roofing, consolidation grouting has been done at the face as well as crown section.
Polyurethane Grouting	Polyurethane grout was injected at the face by drilling holes of length 6 m each.

A considerable and quick geomorphologic re-modelling of the terrain may be seen in the USBRL project region. The ongoing tectonic activities in the Himalayan range cause slope instability events including landslides, debris flows, avalanches, and rock falls to occur frequently. Slope instability issues resembling landslides and debris flows were seen in the vicinity of Tunnel T1, Tunnel T5, and Tunnel T11 (Fig. 7a). Landslides pose a serious risk in the areas around Tunnel T44/45, Tunnel T49, Tunnel T50, Tunnel T74R, and Tunnel T78 located in Ramban. The squeezing ground condition occurred at 35 m from the North Portal of Tunnel T1 (Fig. 7b). The rock mass in the Tunnel T5 area is highly jointed grey dolomite. During the excavation process, a thick shear zone and water inrush were observed on the North Portal of the tunnel (Madhubabu et al. 2016). The presence of a shear zone offers a particularly favourable environment for cavity formation at the tunnel crown (Fig. 7c). As shown in Fig. 7d, during the mucking, a cavity developed on the left side that stretched to the crown of Tunnel T40/41 (Wani and Alamgir 2017). The squeezing was also observed near Southern Portal resulting in the twisting of side walls. During the excavation process of T50 in Ramban, a chimney formed (Fig. 7e) at the collapsed tunnel face (Srivastav et al. 2022). The tunnel T74R consists of Main Tunnel; parallel Escape Tunnel; nineteen cross passages and one Adit. During excavation, tunnel deformation, cavity formation, overbreak of strata, and water seepage was accounted for (Yusoff and Adhikari 2017). The tunnel deformation was observed at the south end portals of both the Main Tunnel and Escape Tunnel (Fig. 7f). Cracks of 5–8 mm were observed at junctions. Due to weak rock mass condition (RMR less than 40), over the break of strata had been observed at various sections along the tunnel. During the Adit excavation, the cavity of approximately 38 m<sup>3</sup> formed in the left-hand crown (towards Srinagar city) due to wedge failure promoted by bedding plain orientation, joints, and seepage.

## 4. Seismic Risk Assessment Of Usbrl Track

The three vertices of the risk triangle are hazard, vulnerability, and exposure to assess the seismic risk of any region or specific structural element (Ansari et al. 2022a). The seismic hazard indicates the earthquake-induced devastation of any area or system. The seismic vulnerability depicts the probability of a region, or any structural constituent of infrastructure projects being damaged during a ground motion with the maximum peak ground acceleration for a defined set of epicentral distance and earthquake magnitude of a specific event (Ansari et al. 2022; Zhang et al. 2022). The exposure represents the socioeconomic value of the region or structure at risk and the projected catastrophic index. The semi-Quantitative Seismic Risk Assessment (SQ-SRA) approach is employed to check the serviceability of any system or part of the system in terms of performance risk (Eskesen et al. 2004; You et al. 2005; Shen et al. 2014; Zhang et al. 2015; Grasso and Soldo 2017; Berge-Thierry et al. 2020; Gómez-Soberón et al. 2022). Each category of risk can be defined as a limit, above which the risk is deemed unacceptable and below which additional risk reduction is not necessary (Eskesen et al. 2004). For different damage states, fragility functions are proposed to understand the level of vulnerability of the structural segment. The risk reduction process involves both active and passive steps. Active steps involve avoiding or reducing hazards, while passive steps involve choosing particular mitigation methods (Zhang et al. 2015). The risk matrices are formed based on the hazard and vulnerability data set. The Seismic Fragility Curves (SFC) are used to represent the vulnerability of structure in both pre and post-seismic stages. These curves establish the conditional probability of a tunnel reaching or exceeding a specified damage state ( $DS_i$ ) for the intensity measure ( $IM$ ) of earthquake motion. SFC can be evaluated using the following Eq. (1) (Argyroudis and Pitilakis, 2012; Andreotti and Lai, 2019; Nguyen et al., 2019; Zhong et al., 2020; Fabozzi et al. 2022). As per Eq. (1), the fragility functions are represented by SFC with a lognormal distribution, assuming that all database uncertainty can be stated just by median uncertainty (Tsindis et al., 2020).

$$P[DS \geq DS_i | IM] = \Phi(\ln IM - \ln IM_{DS_i} / \beta_{total}, DS_i)$$

1

where  $DS$  is the type of damage state in the tunnel lining,  $\Phi$  is the standard normal cumulative distribution function,  $IM_{DS_i}$  is the median threshold value of the seismic intensity measure ( $IM$ ) responsible to form a specific type of damage ( $DS_i$ ) and product of  $\beta_{total}$  and  $DS_i$  give the total lognormal standard deviation describing the total variability associated with each damage state.  $IM_{DS_i}$  and  $\beta_{total}, DS_i$  are the two major parts of seismic fragility curves. For the determination of total lognormal standard deviations, the capacity of tunnel support ( $\beta_C$ ), seismic demand ( $\beta_D$ ), and the estimation of damage state thresholds ( $\beta_{DS}$ ) are regarded as the primary sources of uncertainty. The seismic damages can be grouped into five categories, none ( $DS_0$ ); minor ( $DS_1$ ); moderate ( $DS_2$ ), extensive ( $DS_3$ ), and collapse ( $DS_4$ ). Damage patterns for the tunnel portal and lining are enlisted in Table 6.

**Table 6** Risk assessment chart for railway track serviceability

RISK						
Level	Damage States	Damage Patterns		Health and Safety Risk	Operation Risk	Serviceability
		Tunnel Portal	Tunnel Lining			
Low	None ( $DS_0$ )	-	-	None	Normal operation	Accessible
	Minor ( $DS_1$ )	Small rock falls	Minor cracking and spalling	Possible fall of debris and water leakage		
Medium	Moderate ( $DS_2$ )	Small rock topple and sliding	Small cracking, spalling, and falling	Fall of debris and water leakage	Possible regulation and repair	Accessible with moderate repair
High	Extensive ( $DS_3$ )	Large slumps of soil or rock mass and deep sliding	Large cracking, spalling, and falling	Fall of debris, water leakage, and landslide susceptibility	Not operable with extensive repair	Inaccessible
	Collapse ( $DS_4$ )	Complete collapse and landslide influence	Complete collapse			

In the present study, the serviceability of all phases of the USBRL track was predicted as outcomes of risk assessment considering the SQ-SRA method. The Probabilistic Seismic Hazard Analysis (PSHA) technique, which considers both spatial and temporal uncertainty, was utilised to define the seismic hazard (Cornell, 1968). The central part of Udampur, the bedrock level PGA is estimated as 0.34 g (Ansari et al. 2022c). The Reasi and Ramban have shown the maximum PGA of 0.4 g due to the combined seismic influence of MBT, MCT, and RT.

The probability of experiencing extensive damage to the North Portal of Tunnel T2 is 0.92 for PGA of 0.6 g, as shown in Fig. 8a. The highly jointed and weathered dolomite rock mass at the South Portal of Tunnel T5 indicates the 85% risk of extensive damage, which corresponds to 0.8 g as bedrock PGA produced at RT. The near-site shear zone and strong seismicity characteristics of MCT enhance the risk of both portals of the Tunnel T13 suffering moderate damage. For the Tunnel T40/41, the chance of extensive damage gradually increases when  $PGA > 0.5$  g (Fig. 8b). Due to landslide-prone zones, the chances of extensive damage ( $DS_3$ ) of tunnel portals is very high for the tunnels in P2 among all three major phases. For the Tunnel T44/45, minor damage is twice as likely to occur for the same level of seismic intensity as moderate damage.

As illustrated in Fig. 8c, there is a considerable decline in the damage probability from  $P[DS \geq DS_1 | PGA = 0.7g] = 0.89$  to  $P[DS \geq DS_2 | PGA = 0.7g] = 0.32$ , respectively at the North Portal of Tunnel T80. The vicinity of Tunnel T78 in Phase 33 is extremely vulnerable to slope failure, and debris flow indicates an equal probability of moderate and extensive damages. The Tunnel T80 is around 22.5 km from MCT and MBT, where PGA is anticipated to be more than 0.7 g. From the perspective of structural safety for T80, the tilting of the hazard scenario towards greater PGA and the proximity of the Himalayan thrusts are not looking good. The damage contribution of Tunnel T77D and Tunnel T78 under Phase P33 increases the likelihood of a portal collapse by 50%. The probability of minor damage ( $DS_1$ ), moderate damage ( $DS_2$ ), and extensive damage ( $DS_3$ ) are propounded in Table 7.

**Table 7** Serviceability prediction for all phases of the USBRL project during post-seismic scenarios.

Phases		Tunnels	Probability of Exceedance		Probability of Damage State			Remarks
			DS2	DS3	DS1	DS2	DS3	
P1	P11	T23	0.56	0.35	0.44	0.21	0.35	Accessible
		T25	0.88	0.14	0.12	0.74	0.14	
		T1	0.72	0.21	0.28	0.51	0.21	
	P12	T2	0.94	0.92	0.06	0.02	0.92	Inaccessible
		T3	0.82	0.43	0.18	0.39	0.43	
		T5	0.74	0.72	0.26	0.02	0.72	
	P13	T6	0.92	0.45	0.08	0.47	0.45	Accessible
		T10	0.16	0.13	0.84	0.03	0.13	
		T11	0.18	0.17	0.82	0.01	0.17	
P2	P21	T12	0.15	0.12	0.85	0.03	0.12	Accessible with moderate repair
		T13	0.89	0.27	0.11	0.62	0.27	
		T14	0.75	0.44	0.25	0.31	0.44	
	P22	T15	0.92	0.73	0.08	0.19	0.73	Inaccessible
		T40/41	0.81	0.79	0.19	0.02	0.79	
		T42/43	0.79	0.78	0.21	0.01	0.78	
	P23	T44/45	0.93	0.92	0.07	0.01	0.92	Inaccessible
T46		0.68	0.52	0.32	0.16	0.52		
P3	P31	T47	0.83	0.43	0.17	0.4	0.43	Accessible
		T48	0.76	0.16	0.24	0.6	0.16	
	P32	T49	0.77	0.54	0.23	0.23	0.54	Inaccessible
		T50	0.65	0.63	0.35	0.02	0.63	
		T74R	0.62	0.59	0.38	0.03	0.59	
	P33	T77D	0.87	0.77	0.13	0.1	0.77	Inaccessible
		T78	0.92	0.78	0.08	0.14	0.78	
		T80	0.83	0.71	0.17	0.12	0.71	

The risk matrix of the SQ-SRA is shown in Fig. 9 for each subphase of Phases 2 and 3. The Tunnel T14 of Phase P21 is the most susceptible tunnel, with a 0.44 probability of extensive damage. The highest PGA of 0.83 g is anticipated at a distance of approximately 15 km from RT for this tunnel. The other two tunnels (T12 and T13) under Phase P21 predicted a comparably lower likelihood of damage, which led to this phase's predisposition towards accessibility (Fig. 9a). Because RT and JT are so near to Tunnels T1 and

T2, any seismic activity in this area would undoubtedly have an impact on Phase P1. The combined damage contribution of these three tunnels enables Phase P21 to be accessed with very minor repairs. Tunnel T44/45 has a very high prospect of suffering significant damages since it is situated in a landslide-prone location. There is a strong enough risk that both portals will malfunction. If there is a damage probability greater than 95%, portal collapse, as well as lining cracks, may also occur. The Phase P23 route is inaccessible because of issues with slope instability, weathered rock mass, and a high chance of serious damage close to portal sections. Tunnel T42/43 is the hazard-dominating tunnel having  $P[DS \geq DS_3 | PGA = 0.5g] = 0.77$  for North Portal and  $P[DS \geq DS_3 | PGA = 0.5g] = 0.73$  for South Portal. During the excavation phase, the Tunnels T49, T50, and T74R experienced problems such as chimney formation at a collapsed tunnel face, debris flow, and portal deformation. According to the risk matrix, all three tunnels have a probability of extensive damage of more than 70% (Fig. 9b). Phase 2 is more vulnerable to damage and inaccessible during post-seismic situations as a result of these serious geological issues.

The SQ-SRA method conveyed that there are three categories of serviceability for the USBRL track: accessible (A), inaccessible (B), and accessible with moderate repair (C). The percentage of these three classes, A, B, and C, are shown on the route from Udhampur to Quazigund as 33, 56, and 11, respectively. Figure 10 illustrates the serviceability of railway tracks as a result of the seismic risk assessment of the USBRL project. Udhampur, Chak Rakhwal, Katra, and Reasi are the major railway stations on the track of Phase P1. Phases P11 (Udhampur to Katra) and P13 (Reasi onwards) were discovered to be serviceable (Fig. 10a). Phase P1 displays functional activity with minor ( $DS_1$ ) damage as the main type. Water leaking along the tunnel lining and minor rockfalls close to portal regions are possible, but this phase may be operated normally. The Tunnels along the route of Phase P2 exhibit moderate ( $DS_2$ ) damages and these damages can result in cracks that are 3–30 mm broad and 5–10 m long. The risk matrices highlighted the damage probabilities which indicate that P2 is accessible but repairing is required to mitigate the moderate damages. Subsection 2 is located near MT and is the most challenging phase due to critical geological influences and any repair cost may affect the overall project budget.

The active thrusts in the vicinity of Sangaldan, Arpinchala, Banihal, and Quazigund are MCT, MBT, and BT. The last subsection of the USBRL project is the Quazingund to Baramulla (QZ-BR) segment, including the Sadura, Anantnag, Awantipora, Pampore, Srinagar, Budgam, Mazhom, Pattan, Hamre, and Baramulla railway stations of Kashmir Valley (Fig. 10b). The worst-affected part was found to be Phase 3, which contains two subphases that exhibit a lack of serviceability. Phases P1 and 2 appear to be operable, however, Phase 3 is completely inaccessible (Fig. 10b). It appears that entering P3 from P2 is no longer feasible. The tunnels along the Phase 3 have shown the extensive damage ( $DS_3$ ) of lining and collapse ( $DS_4$ ) of the portals. Additionally, cracks longer than 20 m can be seen in key areas. Collapse ( $DS_4$ ) is the worst kind of damage, as it renders the functionality of the track non-operational without considerable rehabilitation, leading to project failure. At portals, there may be significant landslides and deep sliding, as well as significant spalling and cracking

## 5. Concluding Remarks

The Jammu and Kashmir (J&K) is situated in the Northwestern Himalayas and is frequently subjected to both near-field and far-field earthquake occurrences. The recent 2022 Paktika earthquake ( $M_w=5.9$ ) in Afghanistan and the 2019 Mirpur earthquake ( $M_w=5.6$ ) in Pakistan both prompted researchers to examine the consequences of earthquake dynamics in this area. In the present study, following hazard analysis and vulnerability evaluation, the seismic risk and serviceability of the Udhampur Srinagar Baramulla Rail Link (USBRL) project are assessed under post-seismic scenarios. The goal of this project is the overall growth and development of J&K in terms of practical transportation, industrial farming, tourism, employment, better connectivity with Mainland India, and provision of accessibility to the army and military personnel during emergencies brought on by ongoing geopolitical conflicts in the region. The 345 km long route, which starts in Udhampur and finishes in Baramulla, traverses highly weather and jointed rock masses, folded and faulted tectonic features, shear zones, unstable sloping terrain, and landslide-prone areas. The construction of tunnels and bridges alongside railway tracks is a challenging task that presents significant geological difficulties. At Tunnels T2, T5, T40/41, T50, and T74R, excavation-related phenomena including cavity development, face wall deformation, squeezing, chimney formation, and water leakages were noted. The regions near the locations of T1, T44/45, T49, and T78 have a history of frequent slope failure and debris flow, making them landslide prone. Tunnels T1, T2, T47, T49, T77D, and T80 are in the close vicinity of the MCT, MBT, and BT.

Phase P1, Phase 2, and Phase 3 are classified as accessible, accessible with moderate repair, and inaccessible, according to the risk matrices created using the SQ-SRA approach. The Tunnels in the Katra-Banihal (KT-BN) subsection of this project have demonstrated a significant propensity for extensive damages. Adverse seismic behaviour of tunnels, Phase 2 is no longer in an accessible state. If the portal is repaired and the tunnels are properly lined, this track may be functional. Due to the effects of a high degree of seismicity, landslide susceptibility, weathered rock mass, and close source characterization, Phase 3 is the riskiest track in terms of post-seismic functionality. The seismic performance of Tunnels T48, T74R, and T80 has been triggered by the presence of shear zones, the proximity of the Panjal and Balapur thrusts, and the highly weathered and fractured rock mass beyond the Sangaldan railway station. All associated phases were transferred into an inaccessible category due to the high probability of damage. The tunnel designers, engineers, and risk management authorities may use this study to better understand how different components of the USBRL project will work in post-seismic situations. The risk matrices and maps provided will serve as a valuable tool for increasing public awareness and directing track operations in the event of a major earthquake that occurs in or near J&K in the future.

## Declarations

### Acknowledgments

The earthquake catalogue utilised in this study was provided by the National Center for Seismology (NCS), Ministry of Earth Sciences, New Delhi. The authors appreciate the tunnel data, geotechnical and geological parameters, provided by Northern Railways, Konkan Railway Corporation Limited (KRCL), and Ircon



International. The authors thank for the technical and logistical assistance offered by Patel Engineering Limited. The authors are also grateful to the Divisional Commissioner Office of Jammu and Kashmir for granting special permission for fieldwork in Jammu and Kashmir during the COVID-19 pandemic. The first author is grateful to the Ministry of Education, Government of India for providing fellowship to pursue Ph.D. at the Indian Institute of Technology Delhi (India).

## **Compliance with Ethical Standards**

### **Disclosure of potential conflicts of interest**

We know of no conflicts of interest associated with this publication, and there has been no significant financial support for this work that could have influenced its outcome. As the corresponding author, I confirm that the manuscript has been read and approved for submission by all the named authors.

### **Competing interests**

The authors have no relevant financial or non-financial interests to disclose.

### **Funding**

The authors declare that no funds, grants, or other support were received during the study and preparation of this manuscript.

### **Author contributions**

All authors contributed to the conception, visualisation, methodology, and design aspects of this study. Data collection, data processing, analysis, and materials preparation were performed by Abdullah Ansari. Field surveys in Jammu and Kashmir for the Udhampur Srinagar Baramulla Rail Link (USBRL) project were conducted by Abdullah Ansari and KS Rao. The first draft of the manuscript was written by the first author, and all authors commented on previous versions of the manuscript. All authors read and approved the final manuscript.

### **Data Availability**

The datasets generated during and/or analysed during the current study are available from the corresponding author on reasonable request.

## **References**

1. Ahmad ST, Ahmed R, Wani GF, Sharma P, Ahmed P, Mir RA, Alam JB (2021). Assessing the Status of Glaciers in Upper Jhelum Basin of Kashmir Himalayas Using Multi-temporal Satellite Data. *Earth Systems and Env* 1-15
2. Alam, A., Ahmad, S., Bhat, M.S. and Ahmad, B., 2015. Tectonic evolution of Kashmir basin in northwest Himalayas. *Geomorphology*, 239, pp.114-126.

3. Andreotti, G. and Lai, C.G., 2019. Use of fragility curves to assess the seismic vulnerability in the risk analysis of mountain tunnels. *Tunnelling and Underground Space Technology*, 91, p.103008.
4. Ansari A, Rao KS, Jain AK (2022) Damage Assessment of Tunnels in Seismic Prone Zone During Earthquakes: A Part of Hazard Evaluation, In: Sitharam, T.G., Kolathayar, S., Jakka, R. (Eds), *Earthquakes and Structures, Lecture Notes in Civil Engineering*. Springer, Singapore. pp. 161-169. [https://doi.org/10.1007/978-981-16-5673-6\\_13](https://doi.org/10.1007/978-981-16-5673-6_13)
5. Ansari A., Rao KS, Jain AK (2022e) Damage Analysis of Seismic Response of Shallow Tunnels in Jammu. In: Das, B.B., Hettiarachchi, H., Sahu, P.K., Nanda, S. (Eds.) *Recent Developments in Sustainable Infrastructure (ICRDSI-2020)—GEO-TRA-ENV-WRM. Lecture Notes in Civil Engineering*, vol 207. Springer, Singapore. pp. 611-619 [https://doi.org/10.1007/978-981-16-7509-6\\_47](https://doi.org/10.1007/978-981-16-7509-6_47)
6. Ansari, A., Rao, K.S., Jain, A.K., 2021. Seismic hazard and risk assessment in Maharashtra: a critical review. In: Sitharam T.G., Kolathayar S., Sharma M.L. (Eds.), *Seismic Hazards and Risk, Lecture Notes in Civil Engineering*, vol. 116, Springer, Singapore, pp. 35-45. [https://doi.org/10.1007/978-981-15-9976-7\\_4](https://doi.org/10.1007/978-981-15-9976-7_4)
7. Ansari, A., Rao, K.S., Jain, A.K., 2022b. Seismic Analysis of Shallow Tunnels in Soil Medium. In: Satyanarayana Reddy C.N.V., Muthukkumaran K., Vaidya R. (Eds.), *Stability of Slopes and Underground Excavations, Lecture Notes in Civil Engineering*, vol. 185, Springer, Singapore, pp. 343-352. [https://doi.org/10.1007/978-981-16-5601-9\\_29](https://doi.org/10.1007/978-981-16-5601-9_29)
8. Ansari, A., Zahoor, F., Rao, K. S., & Jain, A. K., 2022c. Seismic hazard assessment studies based on deterministic and probabilistic approaches for the Jammu region, NW Himalayas. *Arabian Journal of Geosciences*, 15(11), 1-26. <https://doi.org/10.1007/s12517-022-10330-z>
9. Ansari, A., Zahoor, F., Rao, K.S. et al. Liquefaction hazard assessment in a seismically active region of Himalayas using geotechnical and geophysical investigations: a case study of the Jammu Region. *Bull Eng Geol Environ* 81, 349 (2022f). <https://doi.org/10.1007/s10064-022-02852-3>
10. Ansari, A., Zahoor, F., Rao, K.S., Jain, A.K., 2022d. Deterministic Approach for Seismic Hazard Assessment of Jammu Region, Jammu and Kashmir. In *Geo-Congress 2022: Geophysical and Earthquake Engineering and Soil Dynamics*, GSP 334, pp. 590-598. <https://ascelibrary.org/doi/abs/10.1061/9780784484043.057>
11. Ansari, A., Zahoor, F., Rao, K.S., Jain, A.K., Riyaz, T.U., 2021a. Seismic Vulnerability of Residential Buildings in Jammu City, Jammu and Kashmir. In *Proc. of the Indian Geotechnical Conference (IGC 2021)*, Trichy, India.
12. Argyroudis, S.A. and Pitilakis, K.D., 2012. Seismic fragility curves of shallow tunnels in alluvial deposits. *Soil Dynamics and Earthquake Engineering*, 35, pp.1-12.
13. Aslam, B., Zafar, A., Qureshi, U.A. and Khalil, U., 2021. Seismic investigation of the northern part of Pakistan using the statistical and neural network algorithms. *Environmental Earth Sciences*, 80(2), pp.1-18.
14. Avouac, J.P., Ayoub, F., Leprince, S., Konca, O. and Helmberger, D.V., 2006. The 2005, Mw 7.6 Kashmir earthquake: Sub-pixel correlation of ASTER images and seismic waveforms analysis. *Earth and Planetary Science Letters*, 249(3-4), pp.514-528.

15. Beghoul, N., Chatelain, J. L., Boughacha, M. S., Benhallou, H., Dadou, R., & Mezioud-Saïch, A. (2010). Seismic empirical relations for the Tellian Atlas, North Africa, and their usefulness for seismic risk assessment. *Pure and Applied Geophysics*, 167(3), 277-321.
16. Berge-Thierry, C., Voldoire, F., Ragueneau, F., Lopez-Caballero, F., & Le Maout, A. (2020). Main achievements of the multidisciplinary SINAPS@ Research Project: Towards an integrated approach to perform seismic safety analysis of nuclear facilities. *Pure and Applied Geophysics*, 177(5), 2299-2351.
17. Choun, Y. S., & Elnashai, A. S. (2010). A simplified framework for probabilistic earthquake loss estimation. *Probabilistic Engineering Mechanics*, 25(4), 355-364.
18. Cilingir, U. and Madabhushi, S.G., 2011. A model study on the effects of input motion on the seismic behaviour of tunnels. *Soil Dynamics and Earthquake Engineering*, 31(3), pp.452-462.
19. Cornell, C.A., 1968. Engineering seismic risk analysis. *Bulletin of the seismological society of America*, 58(5), pp.1583-1606.
20. Dewan A, Islam KM, Fariha TR, Murshed MM, Ishtiaque A et al (2022) Spatial Pattern and Land Surface Features Associated with Cloud-to-Ground Lightning in Bangladesh: An Exploratory Study. *Earth Systems and Environment* 12:1-15
21. Durrani, A.J., Elnashai, A.S., Hashash, Y., Kim, S.J., Masud, A., 2005. The Kashmir earthquake of October 8, 2005: A quick look report. MAE Center CD Release 05-04.
22. Eskesen, S. D., Tengborg, P., Kampmann, J., & Veicherts, T. H. (2004). Guidelines for tunnelling risk management: international tunnelling association, working group No. 2. *Tunnelling and Underground Space Technology*, 19(3), 217-237.
23. Fabozzi, S., Porchia, A., Fierro, T., Peronace, E., Pagliaroli, A., & Moscatelli, M. (2020). Seismic compression susceptibility in dry loose sandy and silty soil in a seismic microzonation perspective. *Engineering Geology*, 264, 105324.
24. Gómez-Soberón, M. C., Pérez, E., Salas, D., & De León-Escobedo, D. (2022). Seismic vulnerability through drift assessment for bridges with geometrical irregularities. *European Journal of Environmental and Civil Engineering*, 26(3), 919-932.
25. Grasso, P., & Soldo, L. (2017). Risk analysis-driven design in tunnelling: the state-of-the-art, learnt from past experiences, and horizon for future development. *Innovative Infrastructure Solutions*, 2(1), 1-23.
26. Gupta, H. and Gahalaut, V.K., 2014. Seismotectonics and large earthquake generation in the Himalayan region. *Gondwana research*, 25(1), pp.204-213.
27. Hashash, Y. M., Kim, B., Olson, S. M., & Ahmad, I. (2012). Seismic hazard analysis using discrete faults in Northwestern Pakistan: Part I—methodology and evaluation. *Journal of Earthquake Engineering*, 16(7), 963-994.
28. Jain, A.K., Lal, N., Sulemani, B., Awasthi, A.K., Singh, S., Kumar, R. and Kumar, D., 2009. Detrital-zircon fission-track ages from the Lower Cenozoic sediments, NW Himalayan foreland basin: Clues for exhumation and denudation of the Himalaya during the India-Asia collision. *Geological Society of America Bulletin*, 121(3-4), pp.519-535.

29. Jangpangi, B.S., Kumar, G., Rathore, D.R. and Dutta, S.A.B.I.R., 1986. Geology of the 'Autochthonous Folded Belt', Jammu & Kashmir Himalaya with special reference to the Panjal Thrust. *Journal Palaeontological Society of India*, 31, pp.39-51.
30. Jayalakshmi, S., Raghukanth, S. T. G., & Rao, B. N. (2018). An XFEM Model for Seismic Activity in Indian Plate. *Journal of Earthquake Engineering*, 22(5), 942-969.
31. Kumar, P., Chamoli, B. P., Kumar, A., & Gairola, A. (2021). Attenuation relationship for peak horizontal acceleration of strong ground motion of Uttarakhand region of central Himalayas. *Journal of Earthquake Engineering*, 25(12), 2537-2554.
32. Lister, G., Kennett, B., Richards, S. and Forster, M., 2008. Boudinage of a stretching slablet implicated in earthquakes beneath the Hindu Kush. *Nature Geoscience*, 1(3), pp.196-201.
33. Madhubabu, N., Kainthola, A. and Singh, T.N., 2016. Use of DruchHyd-2C (Polyurethane) Grout in Himalayan Tunnelling. *INDOROCK*, 2016, p.6th.
34. Malik, J.N. and Mohanty, C., 2007. Active tectonic influence on the evolution of drainage and landscape: geomorphic signatures from frontal and hinterland areas along the Northwestern Himalaya, India. *Journal of Asian Earth Sciences*, 29(5-6), pp.604-618.  
<https://doi.org/10.1016/j.jseaes.2006.03.010>
35. Mazars, J., Grange, S., & Desprez, C. (2011). Seismic risk: Structural response of constructions. *European journal of environmental and civil engineering*, 15(sup1), 223-246.
36. Mehta S.K. and Jolly A. (1989) *Leptomeryx*, an Oligocene Artiodactyl from the Lower Murree of Sial Sui (Kalakot Tehsil), District Rajauri, Jammu and Kashmir. *Current Science*, 58(11), pp. 625-627.
37. Mirzanejad, M., Tran, K. T., McVay, M., Horhota, D., & Wasman, S. J. (2021). Deep void detection with 3D full waveform inversion of surface-based and in-depth source seismic wavefields. *Engineering Geology*, 294, 106407.
38. Mittal, H., Sharma, B., Chao, W. A., Wu, Y. M., Lin, T. L., & Chingtham, P. (2022). A comprehensive analysis of attenuation characteristics using strong ground motion records for the Central Seismic Gap Himalayan Region, India. *Journal of Earthquake Engineering*, 26(5), 2599-2624.
39. Mohanty JK, Guru SR, Dash P, Pradhan PK (2021). Fly ash management and condition monitoring of ash pond. *Earth Systems and Environment* 5(2):445-457
40. Mwafy, A. M., & Elnashai, A. S. (2001). Static pushover versus dynamic collapse analysis of RC buildings. *Engineering structures*, 23(5), 407-424.
41. Mwafy, A. M., & Elnashai, A. S. (2002). Calibration of force reduction factors of RC buildings. *Journal of earthquake engineering*, 6(02), 239-273.
42. Nguyen, D.D., Park, D., Shamsheer, S., Nguyen, V.Q. and Lee, T.H., 2019. Seismic vulnerability assessment of rectangular cut-and-cover subway tunnels. *Tunnelling and Underground Space Technology*, 86, pp.247-261.
43. Pandey, R., Jha, S.K., Alatalo, J.M., Archie, K.M. and Gupta, A.K., 2017. Sustainable livelihood framework-based indicators for assessing climate change vulnerability and adaptation for Himalayan communities. *Ecological indicators*, 79, pp.338-346.

44. Pandita, S.K., Haq, A.U., Bhat, G.M., Singh, Y. and Singh, A., 2021. Identification of active fault topography along the Kishtwar Fault, Jammu and Kashmir, Northwest Himalaya, India. *Environmental Earth Sciences*, 80(4), pp.1-16.
45. Pathier, E., Fielding, E.J., Wright, T.J., Walker, R., Parsons, B.E. and Hensley, S., 2006. Displacement field and slip distribution of the 2005 Kashmir earthquake from SAR imagery. *Geophysical research letters*, 33(20).
46. Rajput, S. S., Jakka, R. S., & Sinvhal, A. (2022). A Spatiotemporal Risk Scenario for a Predictive Earthquake in Western Himalaya. *Journal of Earthquake Engineering*, 1-33.
47. Romshoo, S. A., Rafiq, M., & Rashid, I. (2018). Spatio-temporal variation of land surface temperature and temperature lapse rate over mountainous Kashmir Himalaya. *Journal of Mountain Science*, 15(3), 563-576.
48. Sahana, M., & Sajjad, H. (2017). Evaluating effectiveness of frequency ratio, fuzzy logic and logistic regression models in assessing landslide susceptibility: a case from Rudraprayag district, India. *Journal of Mountain Science*, 14(11), 2150-2167.
49. Sana, H. and Nath, S.K., 2017. Seismic source zoning and maximum credible earthquake prognosis of the Greater Kashmir Territory, NW Himalaya. *Journal of Seismology*, 21(2), pp.411-424.
50. Shah S.M.I. (1977) Stratigraphy of Pakistan: Geological Survey of Pakistan Memoirs, v. 12, p. 1-138.
51. Shen, Y., Gao, B., Yang, X., & Tao, S. (2014). Seismic damage mechanism and dynamic deformation characteristic analysis of mountain tunnel after Wenchuan earthquake. *Engineering Geology*, 180, 85-98.
52. Siddaiah, N.S. and Kumar, K., 2007. Discovery of volcanic ash bed from the basal Subathu Formation (Late Palaeocene–Middle Eocene) near Kalka, Solan District (Himachal Pradesh), Northwest Sub-Himalaya, India. *Current Science*, pp.118-125.
53. Siddaiah, N.S., 2011. Origin of chert breccia at the unconformity between Precambrian Sirban Limestone and Paleogene Subathu Formation: evidence from Kalakot area, J&K Himalaya. *Current Science*, pp.1875-1880.
54. Singh, K., 2010. Tectonic evolution of Kishtwar window with respect to the Main Central Thrust, northwest Himalaya, India. *Journal of Asian Earth Sciences*, 39(3), pp.125-135.
55. Singh, R. B., & Mishra, D. K. (2004). Green tourism in mountain regions-reducing vulnerability and promoting people and place centric development in the Himalayas. *Journal of Mountain Science*, 1(1), 57-64.
56. Srivastav, A., Satyam, N., Rajan, K.S., 2022. Seismic Vulnerability Assessment of Steel Fiber Reinforced Shotcrete Lined (SFRS) Tunnel: A Himalayan Case Study. *Journal of the Geological Society of India*, 98 (2), 185-192. <https://doi.org/10.1007/s12594-022-1957-6>
57. Su, L. J., Hu, K. H., Zhang, W. F., Wang, J., Lei, Y., Zhang, C. L., ... & Zheng, Q. H. (2017). Characteristics and triggering mechanism of Xinmo landslide on 24 June 2017 in Sichuan, China. *Journal of Mountain Science*, 14(9), 1689-1700.

58. Thakur, V.C., 1998. Structure of the Chamba nappe and position of the Main Central Thrust in Kashmir Himalaya. *Journal of Asian Earth Sciences*, 16(2-3), pp.269-282.
59. Tsinidis, G., de Silva, F., Anastasopoulos, I., Bilotta, E., Bobet, A., Hashash, Y.M., He, C., Kampas, G., Knappett, J., Madabhushi, G. and Nikitas, N., 2020. Seismic behaviour of tunnels: From experiments to analysis. *Tunnelling and underground space technology*, 99, p.103334.
60. Wadia, D.N., 1931. The syntaxis of the northwest Himalaya: its rocks, tectonics and orogeny. *Rec. Geol. Surv. India*, 65(2), pp.189-220.
61. Wang, T.T., Kwok, O.L.A., Jeng, F.S., 2021. Seismic response of tunnels revealed in two decades following the 1999 Chi-Chi earthquake (Mw 7.6) in Taiwan: A review. *Engineering Geology*, 287, 106090.
62. Wang, Z. Z., Jiang, Y. J., & Zhu, C. A. (2019). Seismic energy response and damage evolution of tunnel lining structures. *European Journal of Environmental and Civil Engineering*, 23(6), 758-770.
63. Wani AR, Alamgir J (2017) Murre formation and geological problems encountered and mitigation thereof. *Him Prabhat IX:11–23*.
64. Xie, F., Wang, Z., & Liu, J. (2011). Seismic hazard and risk assessments for Beijing–Tianjin–Tangshan, China, area. *Pure and applied geophysics*, 168(3), 731-738.
65. You, K., Park, Y., & Lee, J. S. (2005). Risk analysis for determination of a tunnel support pattern. *Tunnelling and Underground Space Technology*, 20(5), 479-486.
66. Yusoff R, Adhikari KN (2017) Geological studies for construction of T-74R- problems and solutions. *Him Prabhat VIII:28–47*.
67. Zhang, G. H., Jiao, Y. Y., Chen, L. B., Wang, H., & Li, S. C. (2015). Analytical model for assessing collapse risk during mountain tunnel construction. *Canadian Geotechnical Journal*, 53(2), 326-342.
68. Zhang, Y., Wu, Z., Romanelli, F., Vaccari, F., Peresan, A., Zhang, S., ... & Panza, G. F. (2022). Time-dependent seismic hazard assessment based on the annual consultation: A case from the China Seismic Experimental Site (CSES). *Pure and Applied Geophysics*, 1-17.
69. Zhong, Z., Shen, Y., Zhao, M., Li, L., Du, X. and Hao, H., 2020. Seismic fragility assessment of the Daikai subway station in layered soil. *Soil Dynamics and Earthquake Engineering*, 132, p.106044.

## Figures

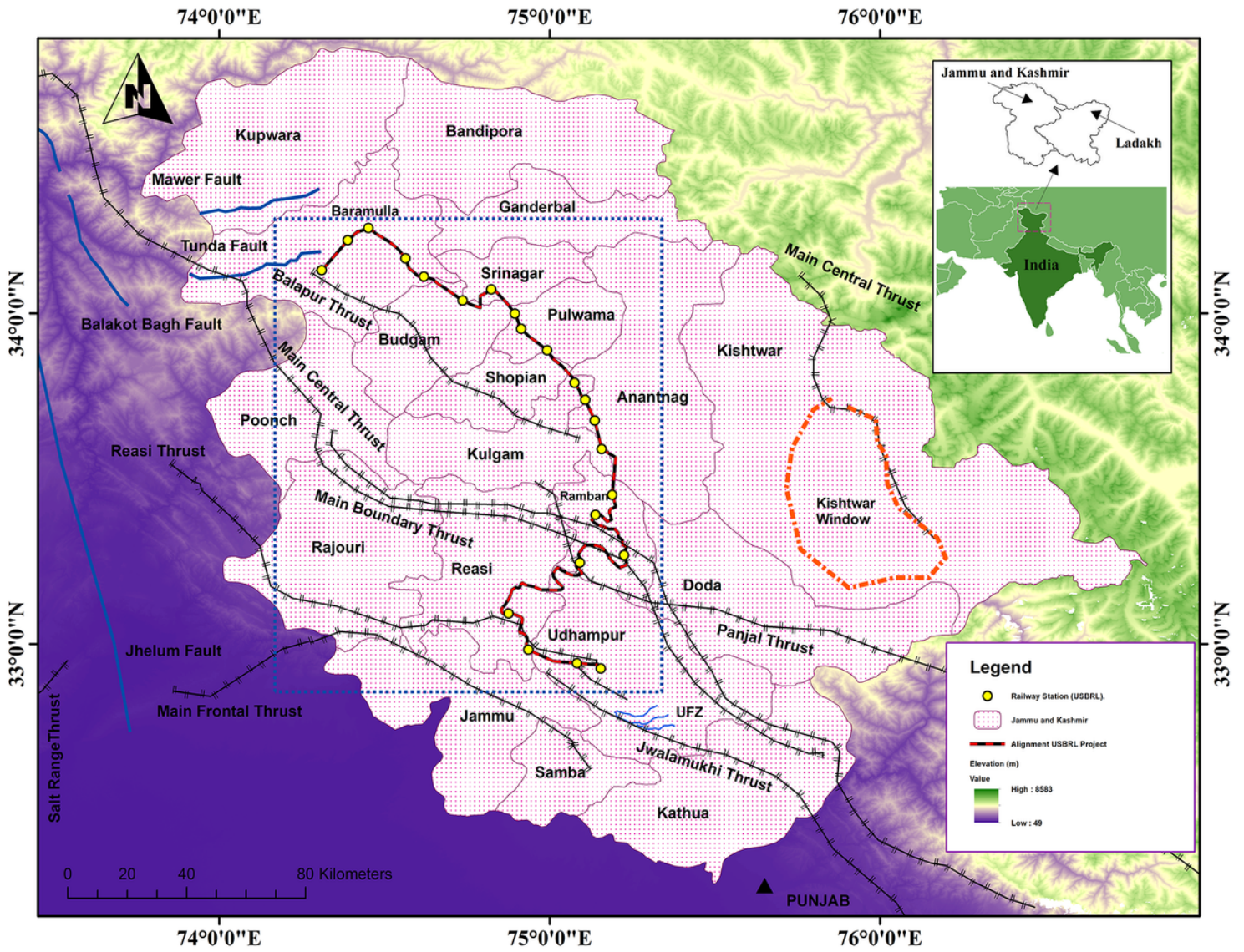


Figure 1

Location of the Udhampur Baramulla Srinagar Rail Link (USBRL) project.



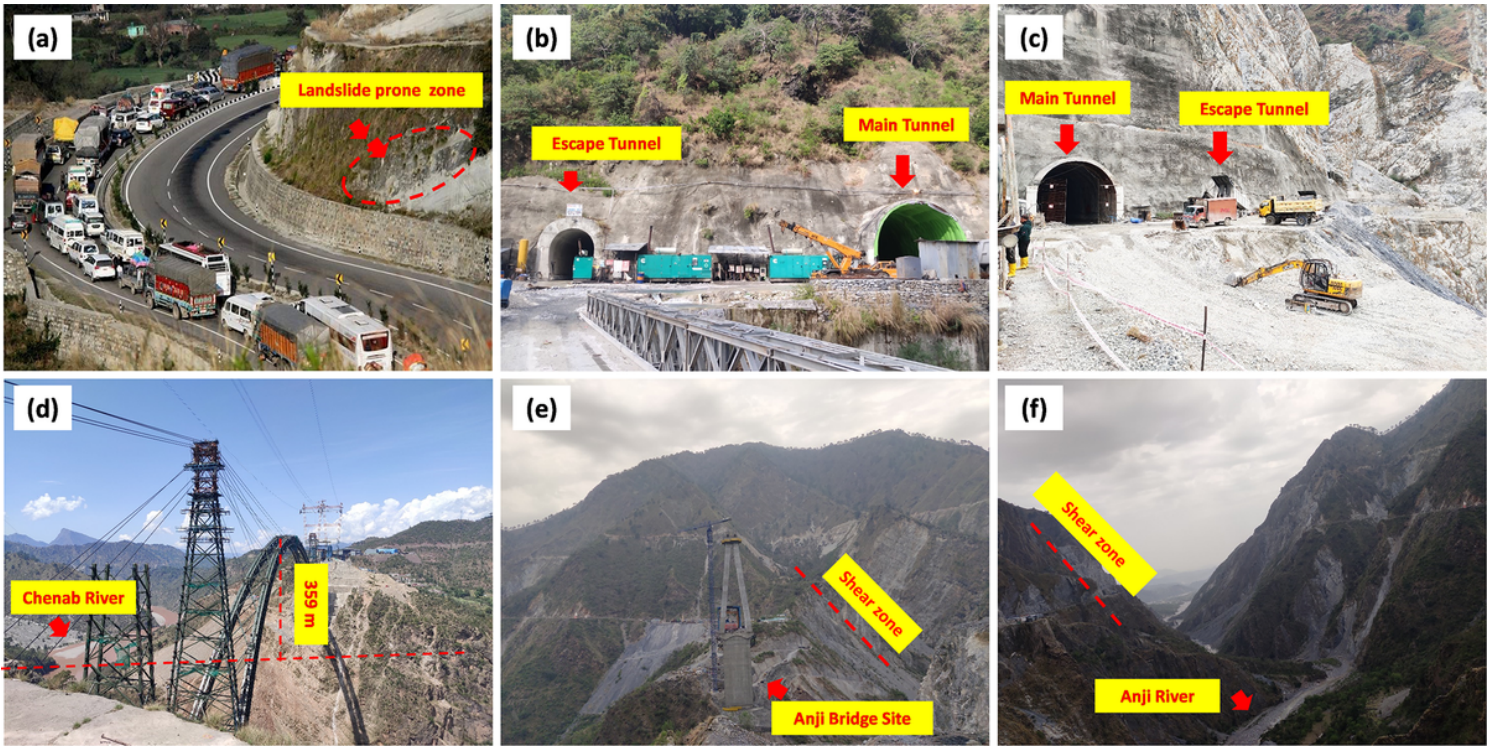


Figure 2

(a) NH1A highway in Jammu and Kashmir, (b) North Portal of Tunnel T2, (c) South Portal of Tunnel T2, (d) Kauri end of Chenab Bridge, (e) Anji Bridge site, and (f) Location near Anji River exposing thinly to thickly layered greyish white cherty dolomite.

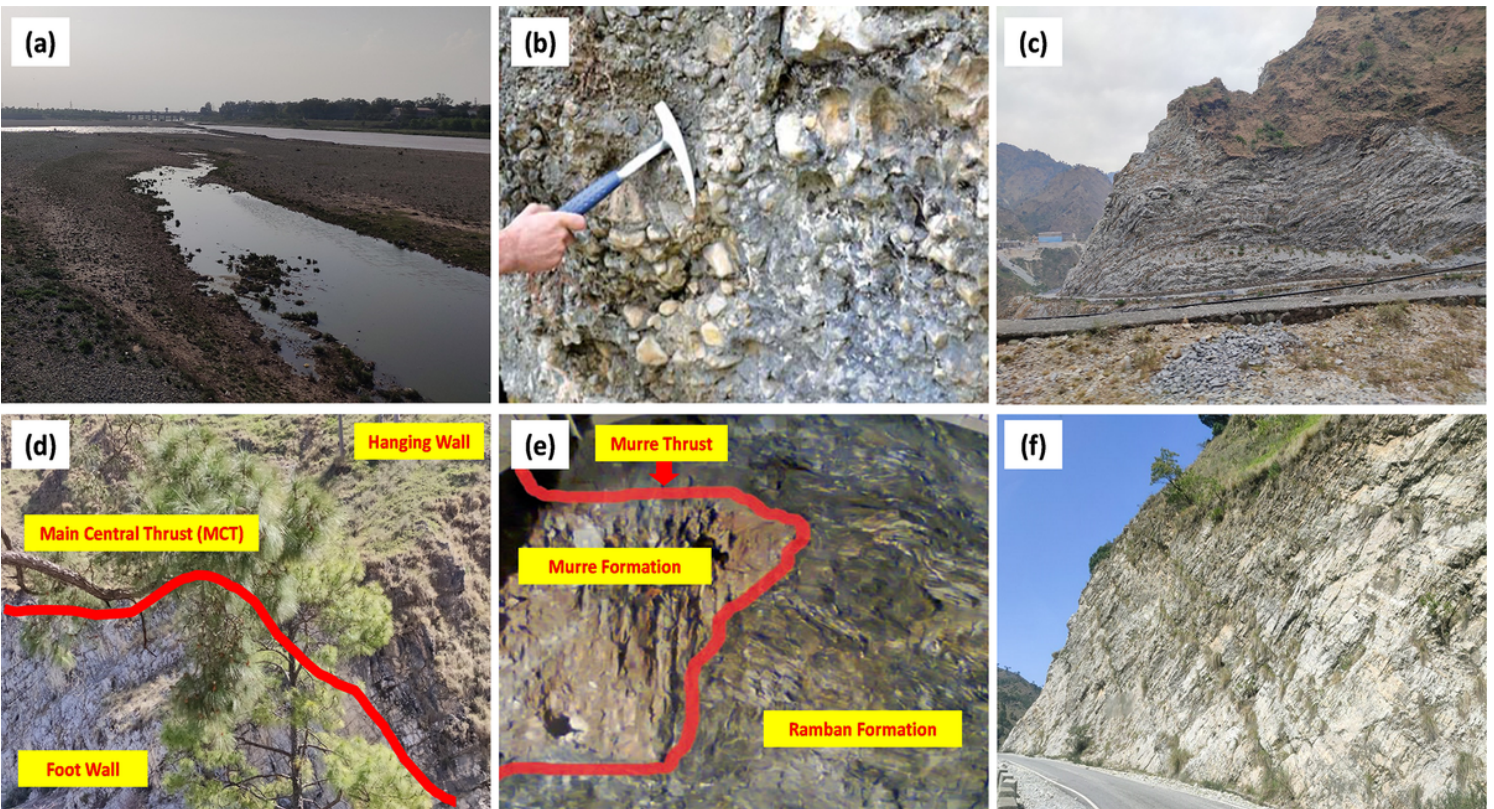


Figure 3



(a) Bank of Tawi River in Jammu, (b) Middle Siwalik Formation in Udhampur showing the outcrops of the conglomerate, (c) Sirban Formation in Reasi showing the outcrops of dolomite, (d) Main Central Thrust (MCT) crossing the area near Southern Portal of Tunnel T49 exhibiting Ramban Formation, (e) Contact between the Murre Formation and Ramban Formation at Tunnel T47 (modified after Wani and Alamgir 2017), and (f) Salkhala Formation showing the outcrops of Phyllites in the Mahu valley, Ramban.

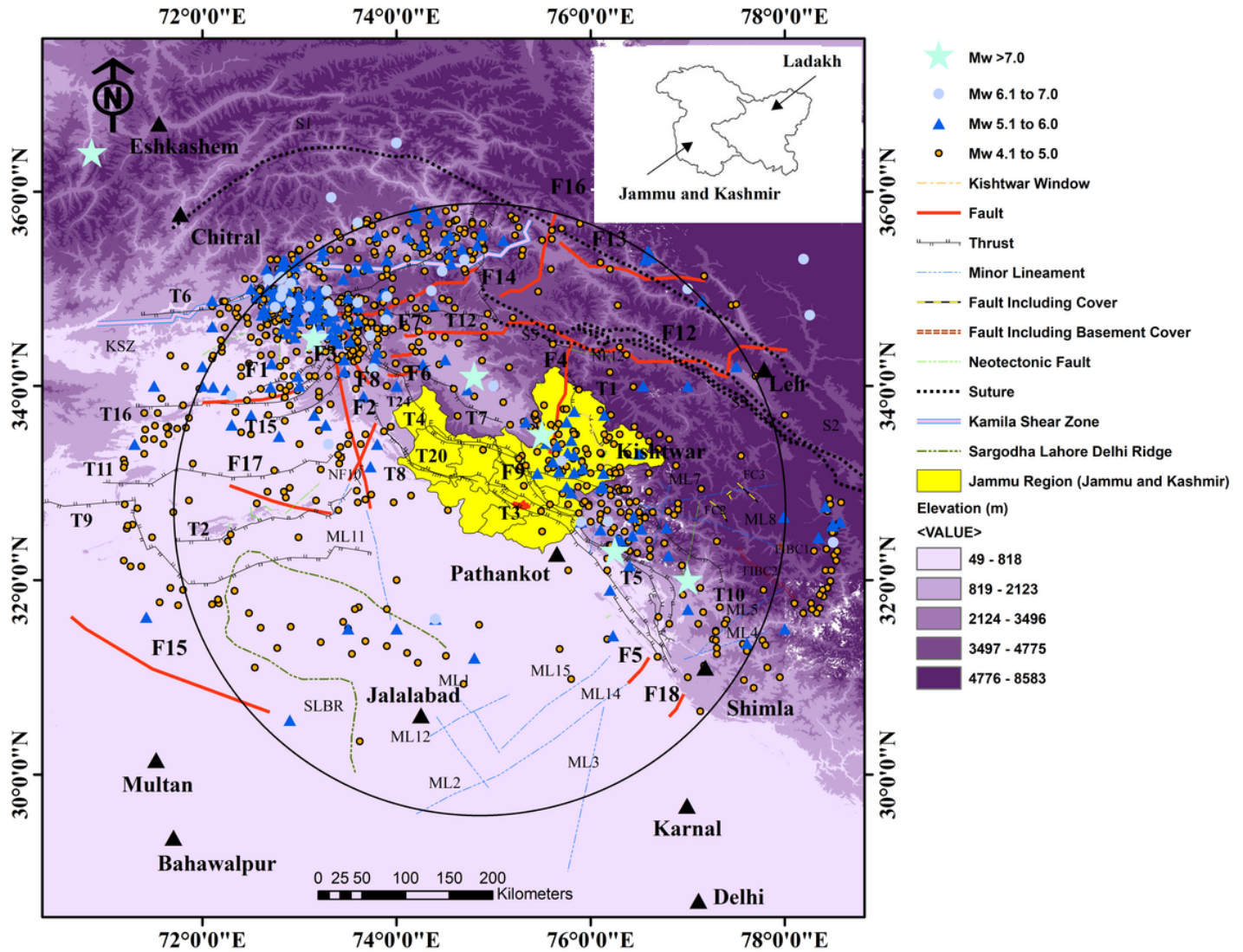


Figure 4

Seismic environment in and around Jammu region with earthquake epicenters of magnitude Mw > 4.0.

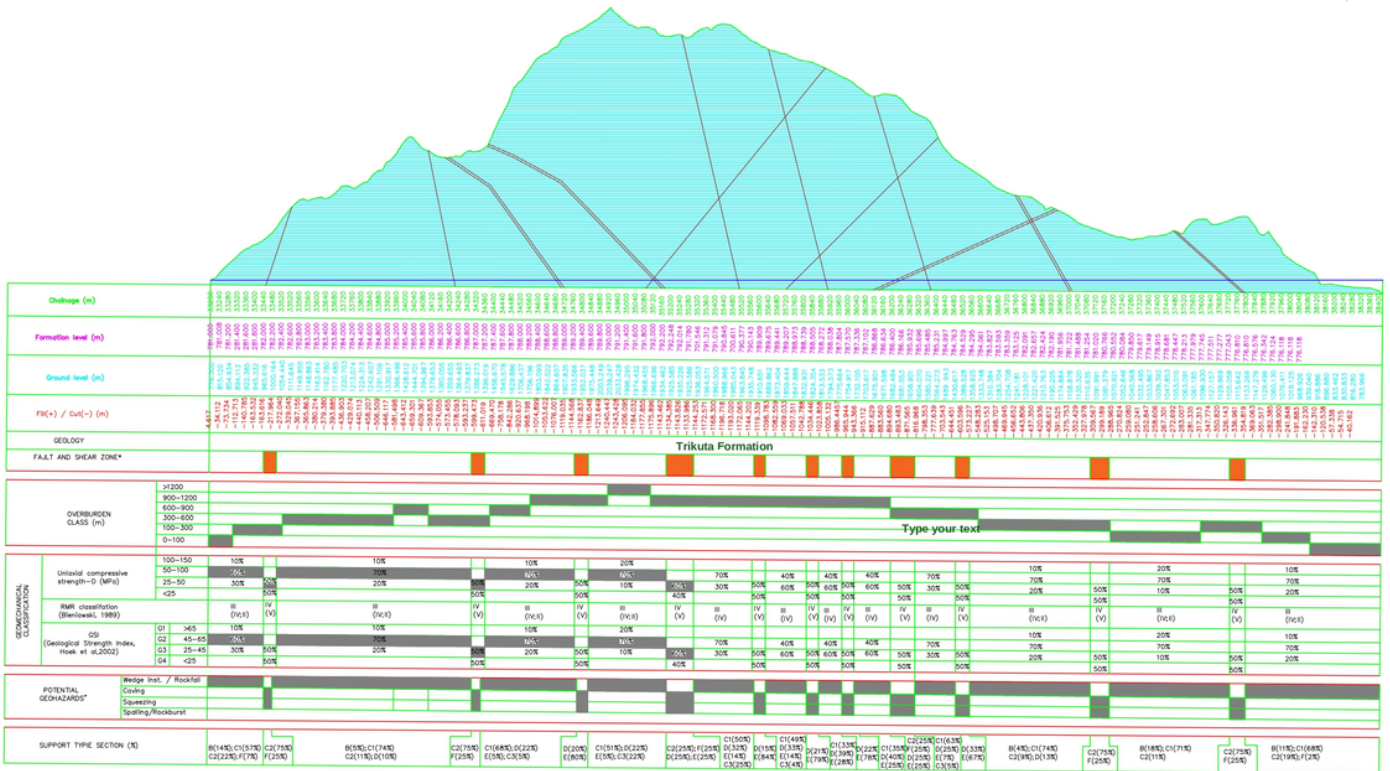


Figure 5

Geological L section of Tunnel T2 in Reasi. In the tunnel section, single and double incline lines indicate thin and thick shear zones respectively. The right end is towards Tunnel T1 while the left end directs towards Anji Khad Bridge.



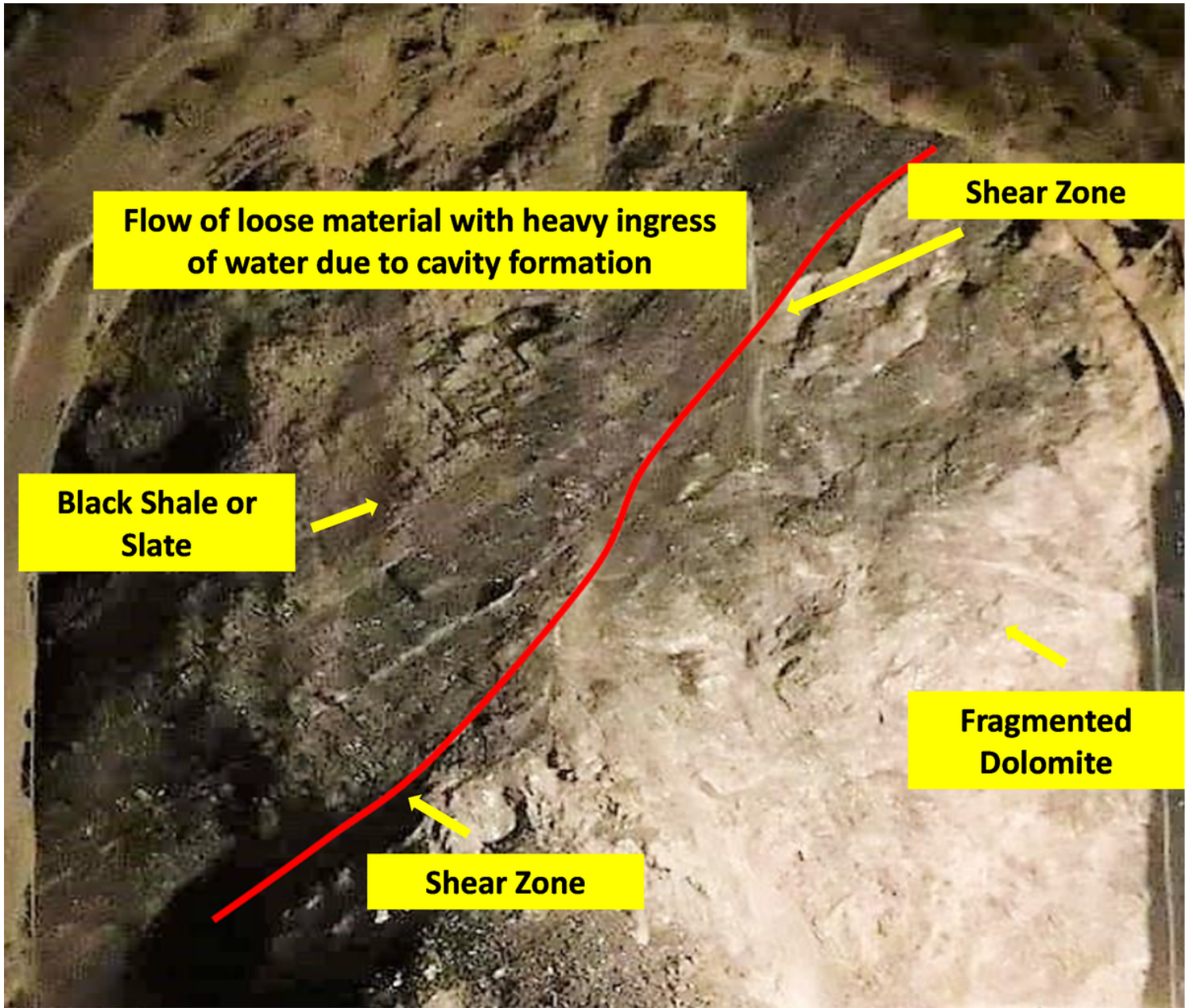
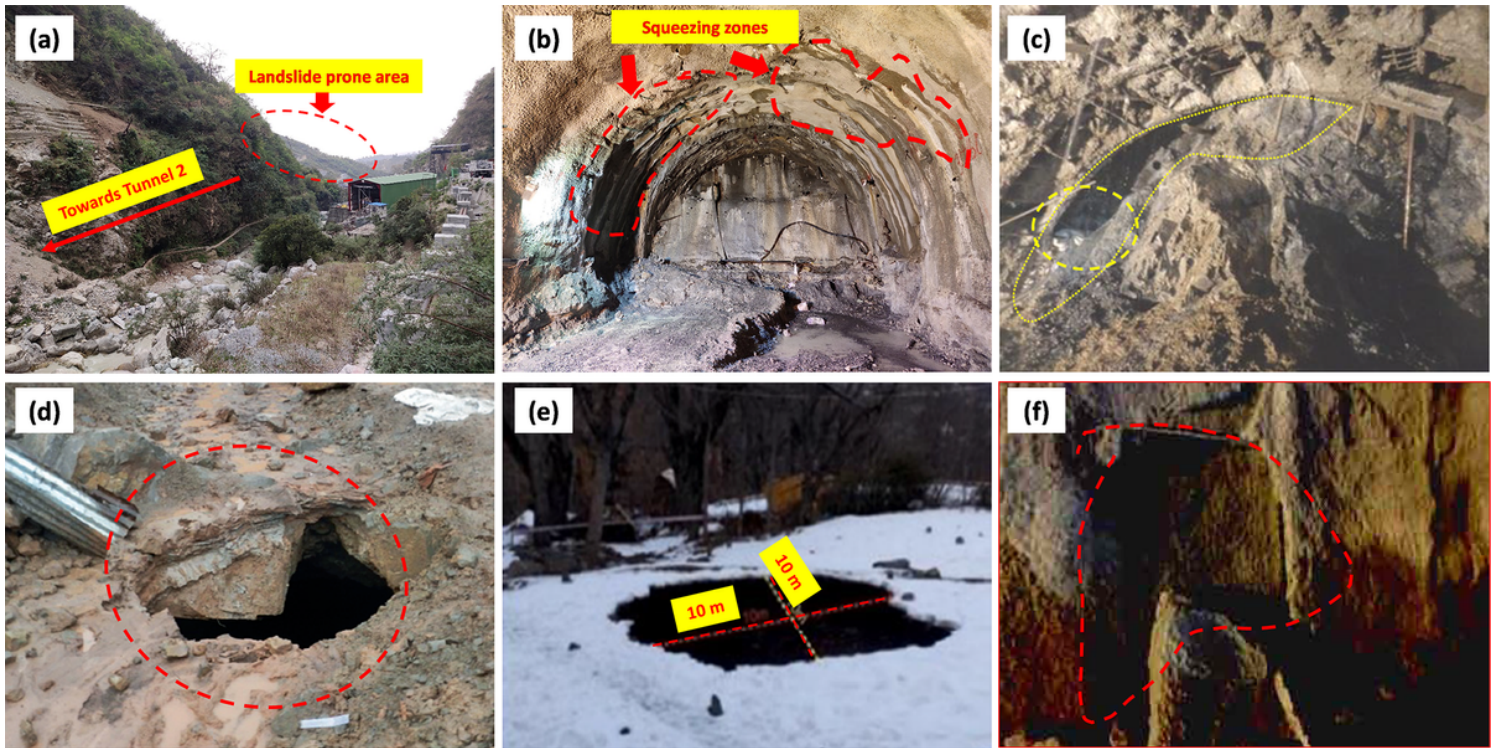


Figure 6

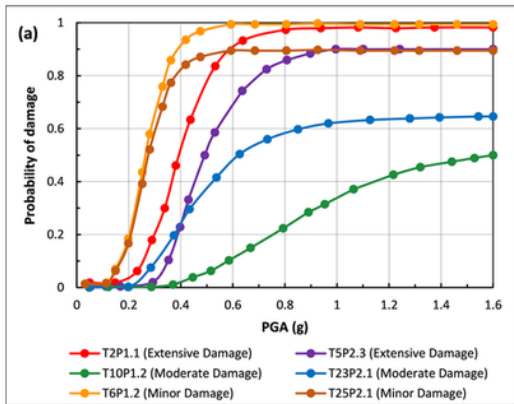
Shear zone separating shale or slate and fragmented dolomite at the Northern face of Tunnel T2.



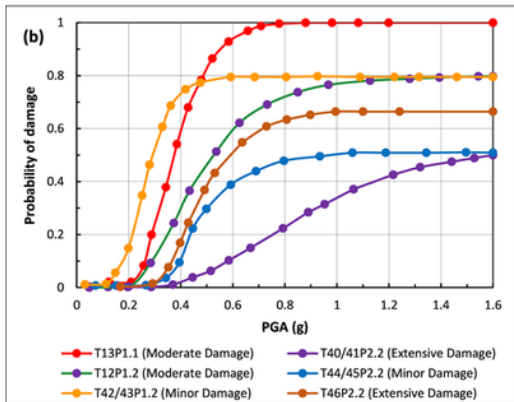
**Figure 7**

(a) Location near South Portal of Tunnel T1 showing highly sheared rock mass and landslide zone, (b) Northern face of Tunnel T1 showing the critical locations of squeezing, (c) Cavity formation at Tunnel T5, (d) Crown level cavity formation at Tunnel T40/41, (e) Chimney formation at tunnel T50 (modified after Srivastav et al. 2022), and (f) Deformation at South Portal of Tunnel T74R (modified after Yusoff and Adhikari 2017).

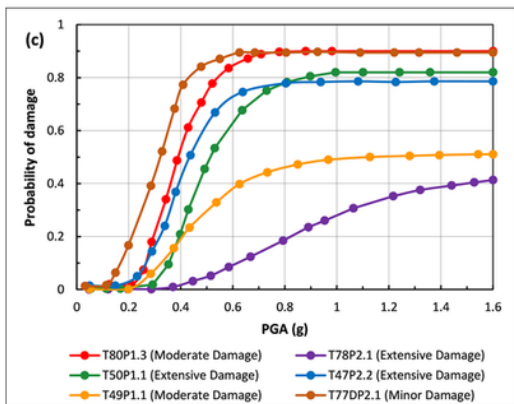




F8a



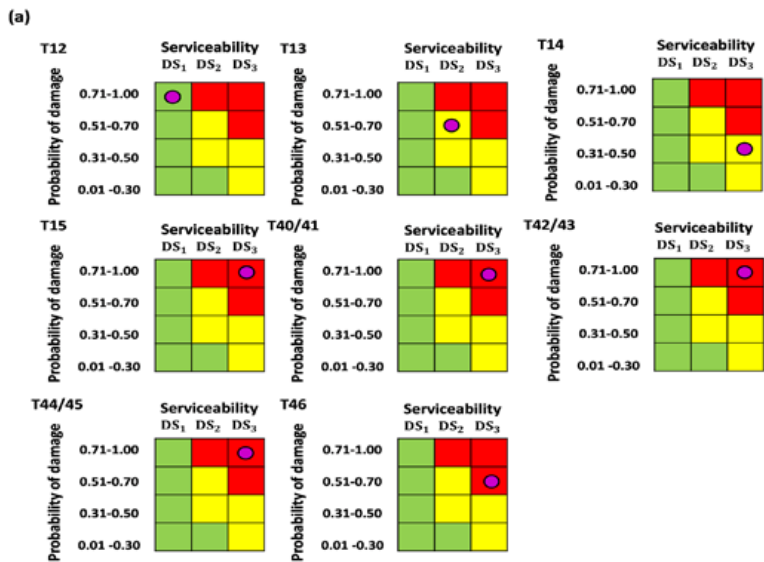
F8b



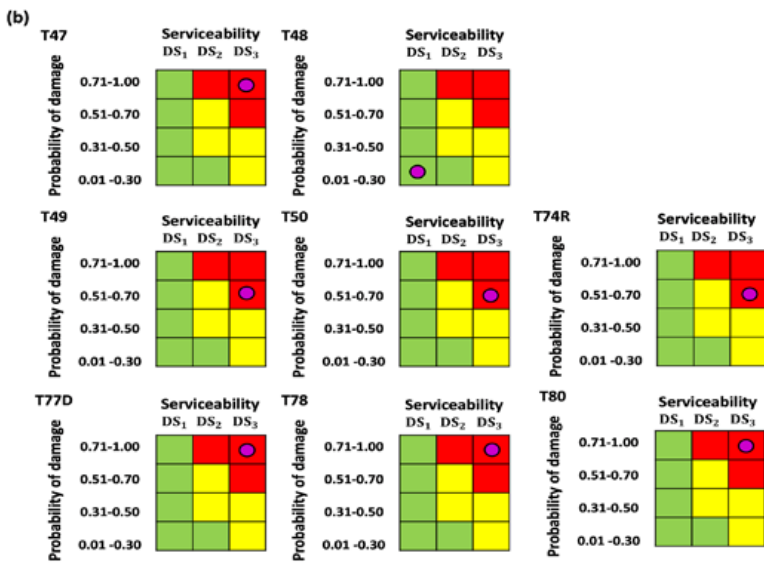
F8c

Figure 8

Seismic fragility curves for tunnel sections along the USBRL track located between the railway stations: (a) Udhampur to Reasi (b) Reasi to Sangaldan, and (c) Sangaldan to Quazigund.



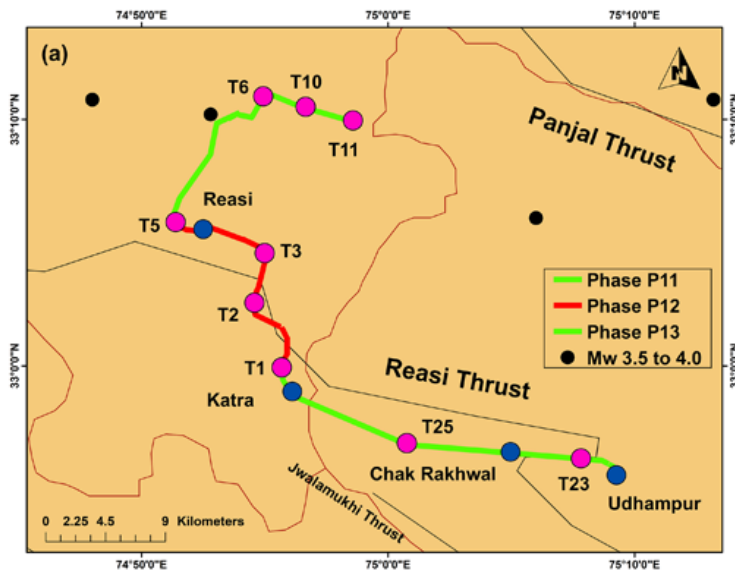
F9a



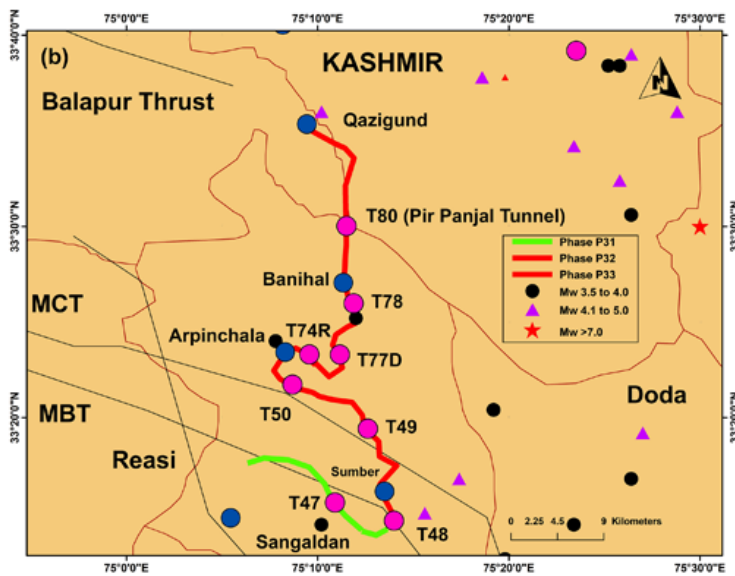
F9b

Figure 9

Risk matrices of Semi-Quantitative Seismic Risk Assessment (SQ-SRA) highlighting the risk for (a) Phase P2, and (b) Phase P3.



F10a



F10b

Figure 10

Post-seismic serviceability of (a) Phase P1, and (b) Phase P3 for the selected tectonic environment and structural integrity of tunnels.